

LA-UR- 01-4282

Approved for public release;
distribution is unlimited.

Title: Probabilistic Fracture Mechanics Analysis
of APT Blanket Tubes

Author(s): Arthur W. Barsell, Kristen T. Kern

Submitted to: American Nuclear Society
November 11-15, 2001
Reno, NV



Los Alamos
NATIONAL LABORATORY

Los Alamos National Laboratory, an affirmative action/equal opportunity employer, operated by the University of California for the U.S. Department of Energy under contract W-7405-ENG-36. By acceptance of this article, the publisher recognizes that the U.S. Government retains a nonexclusive, royalty-free license to publish or reproduce the published form of this contribution, or to allow others to do so, for U.S. Government purposes. Los Alamos National Laboratory requests that the publisher identify this article as work performed under the auspices of the U.S. Department of Energy. Los Alamos National Laboratory strongly supports academic freedom and a researcher's right to publish; as an institution, however, the Laboratory does not endorse the viewpoint of a publication or guarantee its technical correctness.

Probabilistic Fracture Mechanics Analysis of APT Blanket Tubes

Arthur W. Barsell and Kristen T. Kern
General Atomics, 2237 Trinity Drive, Bldg 2, 3rd Floor
Los Alamos, NM 87544

Abstract – A probabilistic fracture mechanics (PFM) model that is specific to the Accelerator Production of Tritium (APT) helium tubes was developed. The model performs Monte Carlo analyses of potential failure modes caused by cyclic stresses generated by beam trips and depressurizations from normal operation, coupled with material aging due to irradiation. Dominant failure probabilities are due to crack through-growth while brittle fracture and ductile tearing have lower probability. Failure mechanisms of global plastic collapse and buckling or crack initiation mechanisms of fatigue or local fracture (upon loss of ductility) have negligible probability. For the population of (7,311) tubes in the APT blanket, the worst-case, annual probability of one tube failing is 3 percent. The probability of 2 or more failures is substantially lower; therefore, unavailability impacts are driven by single failure. The average annual loss of production (unavailability) is below about 0.2 percent. Helium outflow and water inflow rates were characterized for the failures.

I. INTRODUCTION

In the APT design, numerous tubes of aluminum (Al) and stainless steel (SS) surround the target, forming a blanket of 18 modules (tube bundles). During operation, the tubes contain helium under pressure and are cooled by water on the outside. Typical tubes have a SS nozzle at top welded into the SS manifold, SS to Al (bi-metallic) weld, Al to Al weld connecting the nozzle to the body, and lower Al end cap weld. Failure in a tube can cause helium leakage into the water or, under depressurized conditions, water inleakage. Knowledge of the frequency and magnitude of such leaks is needed for unavailability characterization.

II. ANALYTICAL PROCEDURE

Degradation mechanisms analyzed are: 1) crack initiation due to fatigue or local fracture on loss of ductility, 2) crack growth due to fatigue or creep, 3) brittle fracture due to stresses at a crack exceeding the fracture toughness, 4) ductile tearing at the crack, and 5) wall buckling or plastic collapse. The analytical procedure is illustrated in Fig. 1.

At the center is the PFM model that calculates the probabilities of the degradation mechanisms as functions of initial crack depth. Inputs to the procedure are shown by the ovals. Output probabilities of the PFM model are combined with separately-calculated probabilities of crack existence and initial crack depth distribution. This yields the probabilities of failure for key failure mechanisms. Probability distributions for

helium and water leak rates on through-wall growth are also calculated.

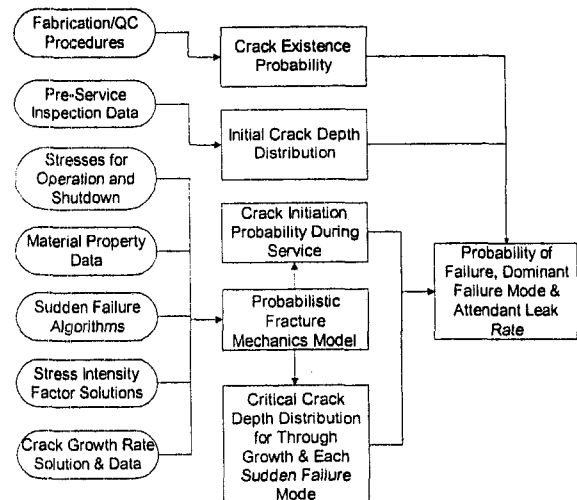


Fig. 1. Block Diagram of the PFM Procedure

The model simulates crack initiation and growth and potential failure caused by cyclic stresses. Cycles occur between steady state conditions of normal operation and beam shutdown or helium depressurization (for tritium harvesting). Semi-elliptical cracks on the inside or outside surfaces of tubes or plates are analyzed using Linear Elastic Fracture Mechanics. Provided as input are membrane and bending stresses acting normal to the crack plane, primary (local) membrane and bending stress intensities, and secondary and peak stress intensities.

The STADIC2 mainframe computer code is used to derive conditional probabilities of failure, given crack existence, for successive increments of initial crack depth from 0 to the wall thickness, h . The code incorporates a deterministic model of the degradation mechanisms into a Monte Carlo sampling scheme to obtain probabilities. A Runge-Kutta numerical integration scheme is used to solve differential equations for crack growth. STADIC2 results are input to Excel spreadsheets to calculate the unconditional probability of failure, based on estimated crack existence probability and probability distributions for initial crack depth, a , and aspect (half length-to-depth, c/a) ratio.

III. PROBABILITY FUNCTIONS

Crack Existence

A range of values for crack existence probability, $P(\text{exist})$, was estimated from literature data for comparable tube fabrication and quality control procedures. Data reviewed were for nuclear reactor tube welds and base metal, a database comprising over 2,100 meters (7,000 feet) of weld seam. The experience data are mainly for steel and Zircaloy tubes, so there is uncertainty extrapolating to the aluminum and stainless steel tubes in the APT blanket. A key parameter is the crack frequency, f^* , defined as the number of cracks per unit length of weld, L , or per tube for base metal. The algorithm for crack existence probability for a specific component in a single tube is:

$$P(\text{exist}) = 1 - e^{-f^* L}. \quad (1)$$

Table I summarizes the calculations of $P(\text{exist})$ for Decoupler tube components (welds and base metal). For welds, the most likely value (mode) of crack frequency, f^* , is a weak function of tube wall thickness, h , according to a formulation by Harris and Dedhia¹, based on data and a model by Chapman²:

$$\text{Mode } f^* = 0.248 - 0.0066 h + 0.0022 h^2. \quad (2)$$

For all welds, the uncertainty range for f^* is taken to be 0.04 to 0.8 per meter, consistent with the data range. Equation 1 simplifies to $P(\text{exist}) \sim f^* L$ because these arguments are much less than one. For cracks in

base metal, a central estimate of $P(\text{exist})$ was obtained from data for N Reactor tubes³ and is shown in Table I.

Initial Crack Depth Distribution

The probability density function (pdf) of initial crack depth in as-fabricated material, $p_0(a)$, given that a crack is present, is represented by an exponential function⁴,

$$p_0(a) = e^{-a/\mu}/(\mu - \mu e^{-h/\mu}), \quad (3)$$

where μ is the mean crack depth. This function must be multiplied by the probability of non-detection, $P_{\text{ND}}(a)$, for a systematic pre-service inspection for cracks.

$$P_{\text{ND}}(a) = \varepsilon + (1 - \varepsilon)e^{-\lambda a}, \quad (4)$$

where λ is the inspection constant and ε is probability of human error. The product of these two functions is the initial crack depth distribution (pdf), $p(a)$. Because the constants μ and λ are uncertain, the function $p(a)$ is given by:

$$p(a) = \int_{\lambda=8}^{20} \int_{\mu=0.064}^{.254} p(a | \lambda, \mu) p(\lambda) p(\mu) d\lambda d\mu. \quad (5)$$

Here, $p(a | \lambda, \mu)$ is the pdf distribution for initial, post-inspection crack depth given specific values of inspection constant and mean crack depth and the limits of integration shown for these parameters pertain to the uncertainty range for the aluminum⁵ locations: Al-Al weld, end cap weld, and base metal. The uncertainty range differs for SS or bi-metallic welds. The algorithm for $p(a | \lambda, \mu)$ is:

$$p(a | \lambda, \mu) = (1/\mu) [\varepsilon e^{-a/\mu} + (1 - \varepsilon) e^{-a\lambda - a/\mu}] / \text{denom}$$

$$\text{denom} = \varepsilon (1 - e^{-h/\mu}) + (1 - \varepsilon) [1 - e^{-h\lambda - h/\mu}] / (1 + \lambda \mu).$$

Also, $p(\lambda)$ and $p(\mu)$ are the pdfs for the values of inspection constant and mean crack depth, respectively. Triangular distributions were used for these quantities, reflecting data from the literature. Numerical integration of the double integral in Eq. 3, using Excel spreadsheets, yielded the pdf for $p(a)$. The complementary cumulative density function, or CCDF, was also calculated for display purposes (CCDF being the probability of exceedance). Figure 2 illustrates the CCDF for initial crack depth at the Al-Al weld.

Table I

Crack Existence Data for Decoupler Tube Components

Component	Crack Frequency f^* (cracks per meter)		Weld Length (meters)	Crack Existence Probability $P(\text{exist})$	
	Mode	Range		Mode	Range
Al-Al weld ($h = 0.9$ mm)	0.24	0.04 to 0.8	0.108	0.026	0.0042 to 0.084
Al end cap weld ($h = 0.9$ mm)	0.24	0.04 to 0.8	0.108	0.026	0.0042 to 0.084
Bi-Metallic weld ($h = 6.9$ mm)	0.20	0.04 to 0.8	0.054	0.011	0.0021 to 0.042
Al base metal ($h = 0.9$ mm)	N/A	N/A	N/A	0.009	0.0015 to 0.03
SS tube/manifold weld ($h = 1.3$ mm)	0.24	0.04 to 0.8	0.036	0.009	0.0014 to 0.028

Initial Aspect Ratio

The ratio of initial crack half-length, c , to depth, a , is based on initial c/a data for steel and Inconel 718 (Ref. 6). To match these data, a lognormal distribution, translated to start at $c/a = 1$ instead of $c/a = 0$, was chosen. This distribution has a median of about 1.5 and a 95th percentile value of about 3.

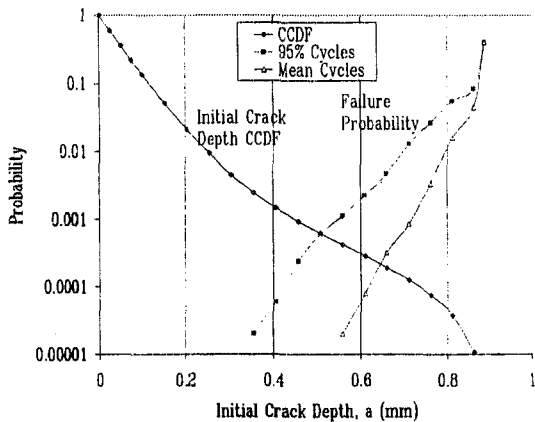


Fig. 2. Initial Crack Depth CCDF and Failure Probability Distributions for Al-Al Weld

Conditional Probability of Failure

This step entails calculating the conditional probability of failure, $P(cf | 1\text{crack})$, given that a crack exists. $P(cf | 1\text{crack})$ is the integral of the product of the pdf for initial crack depth, $p(a)$, and $P(a)$, the failure probability vs. a obtained from STADIC2. Namely,

$$P(cf | 1\text{crack}) = \int_{a=0}^{\infty} P(a) p(a) da. \quad (7)$$

The integral was numerically evaluated via Excel spreadsheets for each tube component. Figure 2 shows the $P(a)$ functions obtained from Monte Carlo analysis for the Al-Al weld.

IV. FAILURE RESULTS FOR TUBE LOCATIONS

In this step, the conditional failure probability, $P(cf | 1\text{crack})$, is combined with the crack existence probability, $P(\text{exist})$, to derive the probability of at least one failure in the time of operation analyzed for a given

location. A range is specified for $P(\text{exist})$, so each end result is stated in terms of a probability range. The single tube failure probability is the sum of location (or component) failure probabilities:

$$P(\text{single tube failure}) = \sum P(\text{exist}) P(cf | 1\text{crack}),$$

where the summation is over all locations (welds and base metal). This process is illustrated for the 95th percentile number of cycles in Table II. The SS tube manifold weld failure probability is negligible.

Results are illustrated in Fig. 3. The lower end cap weld is the greatest contributor to overall tube failure, and base metal is the least contributor.

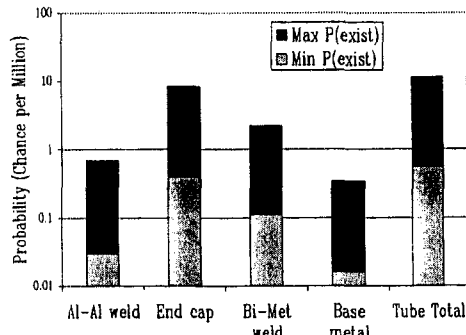


Fig. 3. Component Failure (Through-growth) Probabilities for 95th Percentile Cycles

V. FAILURE RESULTS FOR MULTIPLE TUBES

This step deals with extending failure results from single to multiple tubes. The process is illustrated first for the (688) high-pressure Decoupler tubes that immediately surround the target (modules 1 and 2). These tubes are assumed to be alike in conditions and applied loads. The process is then extended to other tubes in these modules and to other modules.

Table II

Failure Probability vs. Location for High Pressure Decoupler Tube

Location	Crack Existence Probability, $P(\text{exist})$	Conditional Failure Probability, $P(cf 1\text{crack})$	Component Failure Probability Chance per Million
Al-Al weld	0.0042 to 0.084	7.8E-6	0.03 to 0.66
End cap weld	0.0042 to 0.084	9.5E-5	0.4 to 8
Bi-Metallic weld	0.0021 to 0.042	5.1E-5	0.11 to 2.1
Base metal	0.0015 to 0.03	1.1E-5	0.016 to 0.33
		Tube total =	0.56 to 11

Module 1 and 2 Decoupler Tubes

The procedure for calculating the probability of a tube failure in a given bundle of tubes, based on the above results for a single tube, is illustrated in Table III. The example is for the 688 Decoupler tubes in modules 1 and 2. Multiplying the above ranges of $P(\text{exist})$ by 688 yields the range of expected number of initial cracks in all tubes by location. The probability of one tube failing depends on the correlation from tube to tube. Two cases (A and B) are considered below, representing extremes.

Table III

Calculated Annual Probability of a Failure in 688 Tubes

Location	Expected No. of Cracks	Failure Probability	
		Chance per Ten Thousand	
		Case A	Case B
Al-Al weld	2.8 to 58	0.078	0.22 to 4.5
End cap weld	2.8 to 58	0.95	2.7 to 55
Bi-Metallic weld	1.4 to 29	0.51	0.71 to 15
Base metal	1.0 to 21	0.11	0.11 to 2.3
Total, 688 tubes	8 to 166	1.65	3.7 to 77

Case A – perfect tube to tube correlation

Case B – no tube to tube correlation

In case A, failures from tube to tube are assumed perfectly correlated (dependent). Regardless of how many cracks are present, the probability of at least one failure over the operational time is simply equal to $P(\text{cf} | 1\text{crack})$ times the probability that at least one crack is present (which is essentially unity). In this case, the failure probability is $P(\text{cf} | 1 \text{ crack})$, values of which are shown for the 95th percentile number of cycles in the column labeled case A.

In case B, failures from tube to tube are assumed to be not correlated (independent). Then the multiple tube failure probability, for these low numbers (relative to one), is approximately equal to the number of expected cracks times $P(\text{cf} | 1\text{crack})$. This process is the same as

multiplying the single tube failure probability by the number of tubes. The calculation is illustrated for the 95th percentile number of cycles in the last column of the table (labeled case B).

The results pertain to at least one failure over a year of operation. For probabilities of 2 or more failures annually, the process becomes more complicated, involving Poisson functions. The probability of multiple failures is found to be relatively low and can be neglected in the unavailability analysis.

Module Failure Probability Matrix

The above results for high-pressure Decoupler tubes (in modules 1 and 2) were extended in Table IV to other tubes and modules, based on sensitivity calculations. The probability of failure was found to be linearly dependent or proportional to the number of cycles or operational time. Also, the probability of failure varied approximately as the square root of irradiation fluence. Extrapolation from the high-pressure decoupler tubes to other tubes assumes that other tubes, although they have a smaller diameter and same wall thickness, have the same failure probability. This is considered conservative because stresses due to internal pressure are proportional to diameter.

Table IV shows the various modules, the number of tubes (Decoupler and other tubes) in each module, the module service lifetime, peak fluence level, and the probability of a tube failing in the module. Results show that for the total population of 7,311 tubes in the blanket, there is a maximum 18 percent chance that at least one tube will fail (due to slow through-wall growth) in one of the modules before the end of each module's lifetime. The maximum annual risk (sum of module lifetime risk divided by module lifetime) is 3 percent (probability of at least one tube in the blanket failing in a given year).

Table IV

Module Failure Probability Matrix

Module ID	Lifetime yr	Decoupler Tubes	Other Tubes	Fluence dpa	Fluence Factor	Module Lifetime Risk		Facility Life Risk	
						min f*	max f*	min f*	max f*
1	1	329	559	8.4	1	0.00050	0.00977	0.01970	0.32473
2	2	359	636	8.4	1	0.00111	0.02189	0.02205	0.35768
3 to 6	5	0	1024	3.6	0.65	0.00093	0.01830	0.00743	0.13739
13, 14	5	0	544	2.1	0.5	0.00038	0.00748	0.00304	0.05830
16	5	236	504	0.3	0.19	0.00020	0.00387	0.00157	0.03052
15	10	0	384	1	0.35	0.00038	0.00739	0.00150	0.02924
7 to 12	40	0	2400	0.3	0.19	0.00511	0.09545	0.00511	0.09545
17, 18	40	0	336	0.3	0.19	0.00072	0.01404	0.00072	0.01404
Total =		924	6387			0.00932	0.1782	0.06113	0.70426

There is a maximum 70 percent chance that at least one tube will fail in the blanket over the plant life (40 years). Modules 1 and 2 make the largest contributions to the overall facility lifetime risk (see last column of the matrix table) because of high pressure and fluence.

VI. HELIUM AND WATER LEAKAGE

In cases where the crack grows through the wall, a small but significant leak rate of helium from the tube (during normal operation) or water into the tube (during depressurized batch operations) can occur through the crack opening. Calculation of the rates of helium outflow or water inflow requires knowledge of the crack dimensions (length and width) and the stresses acting on the crack. The STADIC2 computer model separately calculates crack growth in the length and depth dimensions. The code starts with an initial aspect ratio, c/a , and continually updates the aspect ratio as the crack grows. At failure, the crack length is simply $2c$ or $2h(c/a)_{fail}$ where the term in parenthesis is the aspect ratio at time of failure (through-growth).

If there is a high local stress at the surface, the crack grows longer (increase in c/a ratio). This occurs at the end cap, where crack lengths at through-wall growth are about 5 times longer compared to other locations.

The width of the crack is proportional to the length and the stress acting to open the crack. The corresponding flow areas (width times length) pertaining to normal operating stresses differ greatly with location because they vary as the square of the length, in addition to stress level differences. Helium outflow and water inflow rates corresponding to the crack flow areas were calculated in the Monte Carlo process. Figure 4 illustrates the helium and water flow rate distributions at the Al-Al weld. Helium flow rates for the end cap are orders of magnitude higher due to higher length of the crack at through-growth. Flow rates for the bi-metallic weld are low because of frictional loss due to the thick wall there.

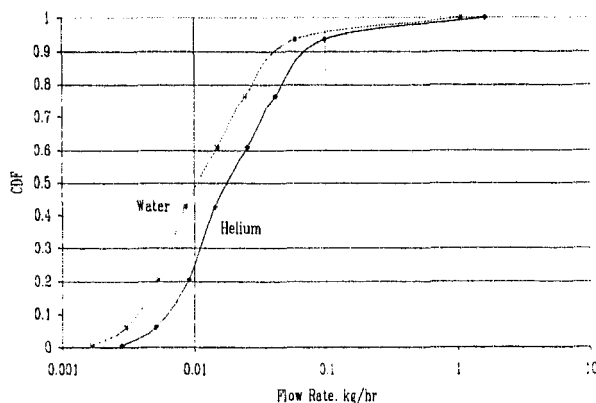


Fig. 4. Cumulative Density Functions for Helium and Water Leak Rates at Al-Al Weld

VII. AVAILABILITY IMPACTS

Impacts of blanket tube failure on availability were estimated using the above failure probabilities as annual failure rates. Repair times were estimated from time and motion studies along with assumptions on operational procedures dealing with failures. The maximum unavailability due to tube failure is found to be about 0.2 percent, a value consistent with APT availability goals.

REFERENCES

1. D.O. HARRIS and D. DEDHIA, 1998. "WinPRAISE 98, PRAISE Code in Windows," Technical Report TR-98-4-1, Engineering Mechanics Technology, Inc., April.
2. O.J.V. CHAPMAN, 1993. "Simulation of Defects in Weld Construction", *PVP-Vol. 251, Reliability and Risk in Pressure Vessels and Piping*, ASME.
3. C. EVERLINE, 1987. "Probabilistic Failure Assessment of the N Reactor Pressure Tubes – Phase III Report", General Atomics Report GA-C19019, November.
4. W. MARSHALL, 1976. "An Assessment of the Integrity of PWR Pressure Vessels," Report by a Study Group, available from H.M. Stationery Office, London, UK.
5. W.D. RUMMEL et al., 1974. "The Detection of Fatigue Cracks by Nondestructive Test Methods," *Materials Evaluation*, 32, No. 6, November, pp. 205-212.
6. S.J. HUDAQ et al., 1990. "A Comparison of Single-Cycle Versus Multiple-Cycle Proof Testing Strategies," NASA Contractor Report 4318, Southwest Research Institute.